ELSEVIER

Journal of Contaminant Hydrology 52 (2001) 109–135

JOURNAL OF Contaminant Hydrology

www.elsevier.com/locate/jconhyd

Modelling the closure-related geochemical evolution of groundwater at a former uranium mine

J.G. Bain [a,*], K.U. Mayer [a], D.W. Blowes [a], E.O. Frind [a], J.W.H. Molson [a], R. Kahnt [b], U. Jenk [b]

[a] *Department of Earth Sciences, University of Waterloo, Waterloo, Ontario, Canada N2L 3G1*
[b] *Wismut GmbH, Jagdschänkenstr. 29, 09117 Chemnitz, Germany*

Abstract

A newly developed reactive transport model was used to evaluate the potential effects of mine closure on the geochemical evolution in the aquifer downgradient from a mine site. The simulations were conducted for the Königstein uranium mine located in Saxony, Germany. During decades of operation, uranium at the former mine site had been extracted by in situ acid leaching of the ore underground, while the mine was maintained in a dewatered condition. One option for decommissioning is to allow the groundwater level to rise to its natural level, flooding the mine workings. As a result, pore water containing high concentrations of dissolved metals, radionuclides, and sulfate may be released. Additional contamination may arise due to the dissolution of minerals contained in the aquifer downgradient of the mine. On the other hand, dissolved metals may be attenuated by reactions within the aquifer. The geochemical processes and interactions involved are highly non-linear and their impact on the quality of the groundwater and surface water downstream of the mine is not always intuitive. The multicomponent reactive transport model MIN3P, which can describe mineral dissolution–precipitation reactions, aqueous complexation, and oxidation–reduction reactions, is shown to be a powerful tool for investigating these processes. The predictive capabilities of the model are, however, limited by the availability of key geochemical parameters such as the presence and quantities of primary and secondary mineral phases. Under these conditions, the model can provide valuable insight by means of sensitivity analyses.

Keywords: Mining; Acid mine drainage; Reactive transport modelling; Metal mobility; Trace mineralogy

* Corresponding author. Tel.: +1-519-888-4567x5369; fax: +1-519-746-3882.
E-mail address: jbain@scimail.uwaterloo.ca (J.G. Bain).

0169-7722/01/$ - see front matter
PII: S0169-7722(01)00155-3

1. Introduction

An important factor to be considered during the operation and decommissioning of a mine site is the potential for contamination of adjacent aquifers and surface-water bodies. Pore water contained within mine tailings and within mine workings often are at low pH and may contain high concentrations of dissolved metals and sulfate. Previous research at mine drainage sites indicates that a complex sequence of acid–base, redox and dissolution–precipitation reactions occur simultaneously as plume water advances through the mine workings, tailings and aquifer (Dubrovsky et al., 1984; Morin et al., 1988; Blowes et al., 1992; Johnson et al., 2000). The geochemical evolution along the flow path is strongly dependent upon the mineralogy of the impacted aquifer and predicting the potential for aquifer contamination due to the release of water with low pH and high metal and sulfate concentrations is difficult at best.

Reactive transport models can be used for investigating the transport of dissolved constituents through the aquifer system, and the reaction of these constituents with the aquifer minerals. Reactive transport modelling has previously been conducted to evaluate chemical transport in mining settings (e.g. Walter et al., 1994a,b; Wunderly et al., 1996; Mayer et al., 1999, 2000; Bain et al., 2000). An investigation by Glynn and Brown (1996) highlighted many of the benefits and limitations of geochemical and reactive transport modelling (PHREEQC: Parkhurst, 1995 and NETPATH: Plummer et al., 1991) at sites with limited spatial information.

The objective of the present study is to show how reactive transport modelling can be used to evaluate the geochemical evolution of the mine water exiting the mine upon flooding and to assess the resulting potential for groundwater contamination of the downgradient aquifer. The former Königstein uranium mine, located in the Saxony region of eastern Germany is used as a case study. The potential for metal transport in the aquifer is evaluated under a variety of possible site conditions by simulating the coupled processes of transport and chemical reactions that are expected to occur as low-pH, high-total dissolved solid (TDS) mine water interacts with aquifer minerals. The simulations were carried out with the general-purpose multicomponent reactive transport model MIN3P (Mayer, 1999). Unfortunately, neither the mineralogy of the aquifer nor the specific secondary minerals that will form as the water interacts with aquifer minerals are well known; the modelling is therefore performed as a sensitivity analysis based on mineralogical limits that are considered reasonable for the site. For predictive modelling, however, detailed mineralogical data would be required. Nevertheless, the study shows that modelling can aid in evaluating the potential impact of mine closure on water quality, and in developing and improving closure plans.

2. Modelling approach

MIN3P is a general-purpose numerical model for reactive transport problems in variably saturated media. The model formulation includes the relevant transport and key geochemical processes influencing mine water migrating through aquifer materials. The

effect of aqueous complexation, oxidation–reduction, ion exchange and mineral dissolution–precipitation reactions on the water and solid phase chemistry can be considered. The model is based on a set of general reactive transport equations, which for fully saturated conditions can be expressed as:

$$\frac{\partial}{\partial t}\left[\phi T_j^{\mathrm{a}}\right] + \nabla\cdot\left[v_{\mathrm{a}} T_j^{\mathrm{a}}\right] - \nabla\cdot\left[\phi D_{\mathrm{a}}\nabla T_j^{\mathrm{a}}\right] + \frac{\partial}{\partial t} T_j^{\mathrm{s}} = Q_j^{\mathrm{in}} + Q_j^{\mathrm{ex}} \qquad j = 1, N_{\mathrm{c}}, \quad (1)$$

where t is time, ϕ is porosity, v_{a} is the particle velocity in the aqueous phase, D_{a} is the dispersion tensor in the aqueous phase, and N_{c} is the number of components in the system. Geochemical equilibrium reactions are directly substituted into the total concentration terms T_j^{a} and T_j^{s}, for aqueous and surface species, respectively. Kinetically controlled reactions are considered in the internal source-sink terms Q_j^{in}, while additions or losses of mass across the domain boundaries are considered in the external source-sink terms Q_j^{ex}. Mineral volume fractions are updated based on the relationship

$$\frac{\mathrm{d}\varphi_i}{\mathrm{d}t} = V_i^{\mathrm{m}} R_i^{\mathrm{m}} \qquad i = 1, N_{\mathrm{m}}, \quad (2)$$

where φ_i is the volume fraction of the mineral phase, V_i^{m} is corresponding molar volume, R_i^{m} defines the overall dissolution–precipitation rate, and N_{m} defines the number of mineral phases.

A global implicit solution method (e.g. Steefel and Lasaga, 1994) based on a direct substitution approach (Yeh and Tripathi, 1989) is employed and the highly non-linear set of equations is linearized using Newton's method. The resulting model formulation is similar to the developments by Steefel and Lasaga (1994) and Lichtner (1996). Except where noted in the text, the thermodynamic database defining geochemical reactions is derived from MINTEQA2 v3.0 (Allison et al., 1991), modified to be consistent with the thermodynamic data compiled for WATEQ4F (Ball and Nordstrom, 1991). The model formulation also includes comprehensive mass balance calculations, which can be used to assess the cumulative release of the metals of concern. A detailed description of the model can be found in Mayer (1999).

3. Königstein mine site description

3.1. Site location and geology

The Königstein mine is located in the Saxony Region of eastern Germany, near the River Elbe, about 20 km south of the City of Dresden (Fig. 1). The study area consists of a series of sandstone aquifers separated by clay-rich aquitards (Fig. 2). The ore body is located in a lower sandstone layer, designated as the fourth aquifer. This aquifer varies from 3- to 15-m thickness (10-m average thickness). An unconfined sandstone unit (3rd aquifer) overlying the 4th aquifer is used as a potable water supply. In general, the 3rd and 4th aquifers are separated by a clay aquitard. Flow through a low permeability clay-rich confining layer below the 4th aquifer is low.

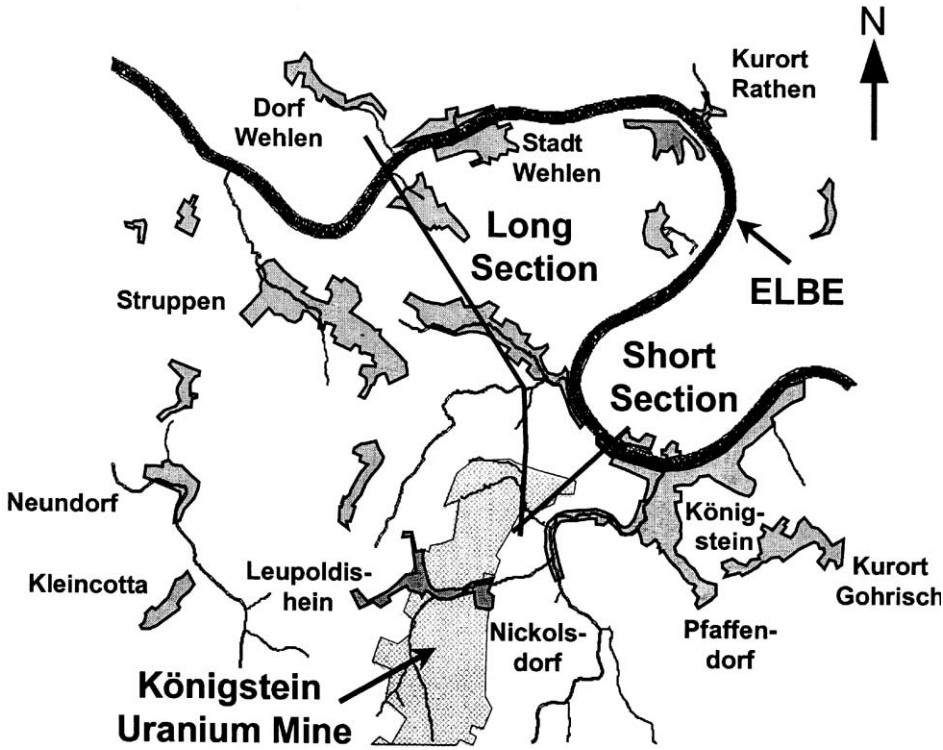

Fig. 1. Königstein mine site location.

3.2. Site history and decommissioning plans

From 1950 through to the end of 1990, uranium ore was extracted at this mine by means of an underground in situ leaching process, which involved passing a sulfuric acid leaching solution through isolated blocks of the ore body. The metal-containing solution was then collected at the base of the mine for processing at surface. To facilitate this operation, and to protect potable water supplies beyond the mine workings, the watertable near the mine (3rd and 4th aquifers) was lowered by pumping. Since closure of the mine in 1990, the low watertable position has been maintained.

Simultaneously with the cessation of mining, the evaluation of decommissioning and rehabilitation possibilities began. One objective of decommissioning is to allow the watertable to rise and thereby to flood the underground mine, in such a way that contamination of the 3rd aquifer and the River Elbe is minimized. As a result of the leaching process, residual pore fluid in the rock is acidic, contains high concentrations of dissolved metals and sulfate, and is in an oxidized state. When the mine is flooded, the 4th aquifer may be contaminated by soluble chemicals contained in the pore water of the mine workings. In addition, the infiltration of acidic mine water may trigger the dissolution of aquifer minerals, releasing contaminants.

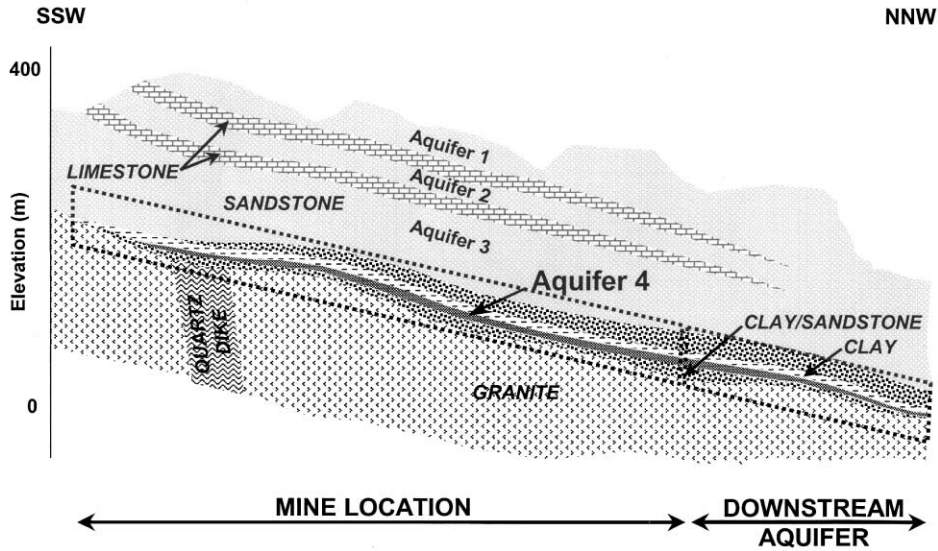

Fig. 2. Schematic cross-section and general geology of the Königstein mine.

3.3. Mineralogy

During mining, core samples of the aquifer material for the determination of uranium grades and for the analysis of bulk mineralogy were collected in the vicinity of the mine. The uranium ore body is low grade, averaging about 0.03 wt.% uranium. The primary ore mineral at the site is uraninite, UO_2, in which uranium is in its reduced state (U(IV)). Downgradient of the mine, the 4th aquifer is composed dominantly of quartz with trace amounts of metal oxides (e.g. gibbsite ($Al(OH)_3$), ferrihydrite ($Fe(OH)_3$), metal sulfides (e.g. pyrite (FeS_2), galena (PbS)), clays and carbonate minerals (Table 1). Unfortunately, because the data requirements of mining geology at this site do not include a detailed mineralogical analysis, the available data are not well suited for geochemical and reactive transport modelling. For example, in the available data, metal oxides and metal sulfides are classified together as a group and the type of clay or

Table 1
General mineralogy of 4th aquifer (Quadersandstein), typical of data available for the site

Composition	Quantity (wt.%)
Quartz	90–96
Feldspar	< 1
Clays	0–3
Metal oxides + metal sulfides	1–2
Carbonates	< 1
Organic material	0–0.1
Accessory	1

carbonate minerals present were not identified. Key data required for reactive transport modelling are therefore unavailable.

3.4. Aquifer aqueous geochemistry

Water collected from well HG 7013 on Feb. 15, 1996 was assumed to be representative of general 4th aquifer water quality. This well is located mid-way between the mine workings and the River Elbe. The composition of the background water is described in Section 5.3 together with the remaining model input parameters.

3.5. Groundwater flow and transport

The groundwater flow system in the complex multi-aquifer system that contains the mine has been modelled in detail by WASY (1995), using the 3D-flow and transport model FEFLOW (Diersch, 1997). On the basis of these 3D-flow simulations, it was determined that a subcrop of the crystalline basement separates flow in the 4th aquifer into two principal flow directions downgradient from the mine. In a northerly direction, the flow path length from the edge of the mine workings to the River Elbe is approximately 5 km ("Long Section" in Fig. 1). In a northeasterly direction, the flow path length from the northern edge of the mine workings to the River Elbe is approximately 1 km ("Short Section" in Fig. 1). Most of the simulations presented here focus on the shorter northeasterly trending flow path, which has higher transport velocities, due to a higher hydraulic gradient. The short flow path, therefore, constitutes the worst-case scenario with respect to the potential environmental impact on the River Elbe. The 4th aquifer does not intersect the River Elbe directly. However, there are indications that discharge from the 4th to the 3rd aquifer, which is hydraulically connected with the River Elbe, occurs within the immediate vicinity of the Elbe.

4. Königstein site conceptual model

4.1. Physical processes

Treatment of the full range of reactive and transport processes in the three-dimensional (3D) context of the actual flow system was found to be impractical due to computer and time limitations. In order to focus on the full range of reactive processes and the complex geochemical evolution of the mine water exiting the mine upon flooding, the spatial domain was simplified to a one-dimensional profile parallel to the direction of groundwater flow. This one-dimensional (1D) conceptual model was considered reasonable because of the large length-to-width ratio of the aquifer (1000–5000 m long, 10 m thick), its relatively uniform thickness, and the resulting uniform flow in the aquifer. Reactive transport processes in the aquifer were assumed to be essentially independent of conditions in neighbouring units and aquifer heterogeneities were neglected at this stage. A more detailed conceptual model based on a 2D cross-section will be considered in later work.

4.2. Geochemical processes

Using estimates of the source water chemistry, mine working and background aquifer mineralogy, a conceptual model of processes that may control the movement of low-pH water and selected dissolved metals at the Königstein site was developed. Previous research at other mine-drainage sites indicates that important solid phases often include carbonates and hydroxides for pH buffering and metal attenuation; sulfates for SO_4 and metal attenuation; and sulfides as potential sources of dissolved metals and as strong reductants (Dubrovsky et al., 1984; Morin et al., 1988; Blowes et al., 1992; Walter et al., 1994a,b; Wunderly et al., 1996; Mayer et al., 1999; Bain et al., 2000). Based on the findings of this previous research, it is reasonable to assume that in a relatively "clean" host rock such as quartz sandstone, influent mine drainage water chemistry is strongly affected by the presence of small concentrations of reactive mineral phases in the aquifer. In developing the site-specific conceptual model, reactions likely to control the movement of Al, Cd, Cr, Fe, Ni, Pb, U, Zn and the anion SO_4 were considered. The basic conceptual model for the behaviour of source water as it advances through the aquifer is described below.

4.2.1. pH, Eh and major-ion controlling reactions

The pH and Eh buffering minerals in aquifers, even when present in seemingly low quantities, affect the mobility of dissolved metals. The carbonate content of the Königstein sandstone is low and poorly defined. In a system where calcite is present, calcite dissolution will buffer the pH of advancing source water, causing an increase in pH, Ca and alkalinity (Eq. (3)),

$$CaCO_3 + H^+ \Leftrightarrow Ca^{2+} + HCO_3^- \qquad \text{Log } K = 1.855 \tag{3}$$

The pH and alkalinity increase at the calcite dissolution front. These increases may result in the formation of secondary mineral phases such as siderite ($FeCO_3$), gibbsite (or amorphous $Al(OH)_3$) and amorphous ferric hydroxide (ferrihydrite, $Fe(OH)_3$; Eqs. (4)–(6)):

$$Fe^{2+} + HCO_3^- \Leftrightarrow FeCO_3 + H^+ \qquad \text{Log } K = 0.120 \tag{4}$$

$$Al^{3+} + 3H_2O \Leftrightarrow Al(OH)_3 + 3H^+ \qquad \text{Log } K = -8.110 \tag{5}$$

$$Fe^{3+} + 3H_2O \Leftrightarrow \text{am-}Fe(OH)_3 + 3H^+ \qquad \text{Log } K = -4.891 \tag{6}$$

The formation of these solids affects the aqueous concentrations of their associated cations (Fe, Al), slowing their migration. Other Al- and Fe(III)-bearing phases such as am-$Al(OH)_3$, or goethite (FeOOH) may form in place of, or in addition to these minerals. Because the solubility of these minerals differs from the solubility of gibbsite and ferrihydrite, the mobility of the associated dissolved metals will also vary.

Gypsum ($CaSO_4 \cdot 2H_2O$) may also precipitate due to increased Ca-concentrations at the calcite dissolution front, thereby providing an upper limit on dissolved Ca and SO_4 concentrations (Eq. (7)).

$$Ca^{2+} + SO_4^{2-} + 2H_2O \Leftrightarrow CaSO_4 \cdot 2H_2O \qquad \text{Log } K = 4.580 \tag{7}$$

Previous research in areas affected by mine drainage indicates that with the eventual arrival of low-pH source water, the primary and secondary carbonate and hydroxide minerals dissolve in a consistent sequence (Dubrovsky et al., 1984; Morin et al., 1988; Blowes et al., 1992; Johnson et al., 2000). With the initial influx of source water into the aquifer, calcite located near the source dissolves, maintaining the pH near 6. When calcite has been depleted at a location, secondary siderite will begin to dissolve, buffering the pH near 5. After siderite is depleted, any gibbsite present will begin to dissolve, resulting in a pH near 4. After gibbsite is depleted, any ferrihydrite present will dissolve, buffering the pH near 3. These dissolution reactions consume H^+, but release metals, which may subsequently reprecipitate farther along the flow path or in the surface water environment.

Previous research at mine drainage sites indicates that the basic ferric sulfate mineral jarosite ($KFe_3(SO_4)_2(OH)_6$) precipitates under pH conditions lower than 2.3 (Eq. (8)).

$$K^+ + 3Fe^{3+} + 2SO_4^{2-} + 6H_2O \Leftrightarrow KFe_3(SO_4)_2(OH)_6 + 6H^+ \qquad \log K = 9.210 \tag{8}$$

4.2.2. Uranium mobility

Of particular concern at the Königstein site is the mobility of uranium. As low-pH, high-Eh source water advances into the aquifer, high concentrations of dissolved oxidized species in the source water (e.g. Fe(III) where Fe(III) = the sum of all dissolved ferric iron-bearing species) dissolves (oxidizes) uraninite present in the aquifer. The oxidation and dissolution of uraninite by source-water Fe(III) is shown in Eq. (9),

$$UO_2 + 2Fe^{3+} \Leftrightarrow UO_2^{2+} + 2Fe^{2+} \qquad \text{Log } K = 11.96 \tag{9}$$

This reaction will cause an increase in dissolved uranium and ferrous iron concentrations. In the presence of reduced mineral phases (i.e. redox buffers), such as pyrite (or other sulfides), there will be a competition for Fe(III) contained in the source water, as pyrite may also be oxidized by Fe(III),

$$FeS_2 + 14Fe^{3+} + 8H_2O \Leftrightarrow 15Fe^{2+} + 2SO_4^{2-} + 16H^+ \qquad \text{Log } K = 96.78 \tag{10}$$

In this case, Fe(III) is not available to oxidize uraninite, and UO_2^{2+} concentrations remain low. Ferrous iron concentrations, however, increase from the source-water levels, increasing the possibility of acidification of receiving surface water bodies, if these high concentrations of Fe(II) are discharged to the surface water environment (Eq. (11)).

$$2Fe^{2+} + 1/2O_2 + 5H_2O \Leftrightarrow 2Fe(OH)_3 + 4H^+ \qquad \text{Log } K = 7.198 \tag{11}$$

Other oxidized dissolved species, including UO_2^{2+}, may be reduced by sulfide minerals in the aquifer. For example, the reduction of UO_2^{2+} by pyrite may cause the precipitation of uraninite,

$$FeS_2 + 7UO_2^{2+} + 8H_2O \Leftrightarrow 7UO_2 + 2SO_4^{2-} + Fe^{2+} + 16H^+ \qquad \text{Log } K = -20.91 \tag{12}$$

Table 2 lists the equilibrium constants for aqueous species in the uranium system.

Table 2
Thermodynamic properties for aqueous uranium species included in the simulations

Reaction	Log K
$U^{4+} + H_2O - H^+ \leftrightarrow UOH^{3+}$	-0.54[a]
$U^{4+} + 2H_2O - 2H^+ \leftrightarrow U(OH)_2^{2+}$	-2.27[a]
$U^{4+} + 3H_2O - 3H^+ \leftrightarrow U(OH)_3^+$	-4.94[a]
$U^{4+} + 4H_2O - 4H^+ \leftrightarrow U(OH)_{4(aq)}$	-8.50[a]
$U^{4+} + 5H_2O - 5H^+ \leftrightarrow U(OH)_5^-$	-13.12[b]
$U^{4+} + F^- \leftrightarrow UF^{3+}$	9.30[a]
$U^{4+} + 2F^- \leftrightarrow UF_2^{2+}$	16.22[a]
$U^{4+} + 3F^- \leftrightarrow UF_3^+$	21.60[a]
$U^{4+} + 4F^- \leftrightarrow UF_{4(aq)}$	25.50[a]
$U^{4+} + 5F^- \leftrightarrow UF_5^-$	27.01[a]
$U^{4+} + 6F^- \leftrightarrow UF_6^{2-}$	29.10[a]
$U^{4+} + Cl^- \leftrightarrow UCl^{3+}$	1.72[a]
$U^{4+} + SO_4^{2-} \leftrightarrow USO_4^{2+}$	6.58[a]
$U^{4+} + 2SO_4^{2-} \leftrightarrow U(SO4)_{2(aq)}$	10.50[a]
$U^{4+} + PO_4^{3-} + H^+ \leftrightarrow UHPO_4^{2+}$	24.44[b]
$U^{4+} + 2PO_4^{3-} + 2H^+ \leftrightarrow U(HPO_4)_{2(aq)}$	46.83[b]
$U^{4+} + 3PO_4^{3-} + 3H^+ \leftrightarrow U(HPO_4)_3^{2-}$	67.56[b]
$U^{4+} + 4PO_4^{3-}\ 4H^+ \leftrightarrow U(HPO_4)_4^{4-}$	88.48[b]
$UO_2^{2+} + H_2O - H^+ \leftrightarrow UO_2OH^+$	-5.20[a]
$2UO_2^{2+} + 2H_2O - 2H^+ \leftrightarrow (UO_2)_2(OH)_2^{2+}$	-5.62[a]
$3UO_2^{2+} + 5H_2O - 5H^+ \leftrightarrow (UO_2)_3(OH)_5^+$	-15.55[a]
$UO_2^{2+} + CO_3^{2-} \leftrightarrow UO_2CO_{3(aq)}$	9.63[a]
$UO_2^{2+} + 2CO_3^{2-} \leftrightarrow UO_2(CO_3)_2^{2-}$	17.00[a]
$UO_2^{2+} + 3CO_3^{2-} \leftrightarrow UO_2(CO_3)_3^{4-}$	21.63[a]
$UO_2^{2+} + F^- \leftrightarrow UO_2F^+$	5.09[a]
$UO_2^{2+} + 2F^- \leftrightarrow UO_2F_{2(aq)}$	8.62[a]
$UO_2^{2+} + 3F^- \leftrightarrow UO_2F_3^-$	10.90[a]
$UO_2^{2+} + 4F^- \leftrightarrow UO_2F_4^{2-}$	11.70[a]
$UO_2^{2+} + Cl^- \leftrightarrow UO_2Cl^+$	0.17[a]
$UO_2^{2+}\ SO_4^{2-} \leftrightarrow UO_2SO_{4(aq)}$	3.15[a]
$UO_2^{2+} + 2SO_4^{2-} \leftrightarrow UO_2(SO_4)_2^{2-}$	4.14[a]
$UO_2^{2+} + PO_4^{3-} + H^+ \leftrightarrow UO_2HPO_{4(aq)}$	20.21[a]
$UO_2^{2+} + 2PO_4^{3-} + 2H^+ \leftrightarrow UO_2(HPO_4)_2^{2-}$	43.44[a]
$UO_2^{2+} + PO_4^{3-} + 2H^+ \leftrightarrow UO_2H_2PO_4^+$	22.64[b]
$UO_2^{2+} + 2PO_4^{3-} + 4H^+ \leftrightarrow UO_2(H_2PO_4)_{2(aq)}$	44.70[b]
$UO_2^{2+} + 3PO_4^{3-} + 6H^+ \leftrightarrow UO_2(H_2PO_4)_3^-$	66.245[a]
$UO_2^{2+} + H_4SiO_{4(aq)} - H^+ \leftrightarrow UO_2H_3SiO_4^+$	-2.40[b]

[a] Source: WATEQ4F.
[b] Source: MINTEQA2.

4.2.3. Trace metal mobility

The mobility of the trace metals Cd, Cr and Zn is also of specific concern for this study. These metals are present in the source water and have been detected in whole rock analyses. Mineralogical studies, however, have not identified mineral sources of these metals at Königstein, potentially a result of low mineral contents. The movement of these metals may be tied to the movement of the low pH water. The movement of Cr is also sensitive to the redox state of the water, as it is typically soluble in the Cr(VI)

state and sparingly soluble in the Cr(III) state. Some potential secondary minerals that may form as the aquifer is flooded include otavite ($CdCO_3$), $Cr(OH)_3$ and smithsonite ($ZnCO_3$), as indicated by equilibrating the source water with calcite. MINTEQA2 calculations showed that precipitation of these minerals is favoured under calcite-buffered, near-neutral pH conditions. Direct precipitation of metal carbonates is unlikely, however. It is more likely that hydrous metal carbonates will precipitate, followed by slow recrystallization to less hydrous forms. For simplicity, only the anhydrous metal carbonates were considered in these simulations. As low pH water infiltrates, sequential precipitation and dissolution of otavite, $Cr(OH)_3$ and smithsonite at the calcite dissolution front affects the concentrations of Cd, Cr and Zn. At the mineral dissolution fronts, Cd, Cr and Zn concentrations increase to maximum values. However, these maximum values subsequently decrease due to downgradient reprecipitation of the corresponding metal-bearing minerals in the presence of calcite.

In addition, Ni and Pb are heavy metals of potential concern, having been detected in whole rock analyses. Sources of Ni and Pb in the aquifer include millerite (NiS) and galena (PbS). These sulfide phases may dissolve and release Ni and Pb as oxidizing source water moves through the aquifer. Under neutral to basic pH conditions, precipitation of $Ni(OH)_2$ may limit dissolved Ni concentrations. If dissolved SO_4 concentrations are high, anglesite precipitation may limit dissolved Pb concentrations. No other sources or sinks of Ni or Pb were identified by the mineralogical investigations at Königstein.

With the exception of $Cr(OH)_3$ (MINTEQA2), the thermodynamic parameters of the primary and secondary minerals included in the investigation were defined from the database of WATEQ4F (Table 3).

Table 3
Equilibrium constants for primary and secondary minerals included in the investigation

Mineral	Log K
$Ca^{2+} + CO_3^{2-} \leftrightarrow$ Calcite	8.475[a]
$Cr^{3+} + 3H_2O - 3H^+ \leftrightarrow Cr(OH)_3$	0.75[b]
$Ca^{2+} + Mg^{2+} + 2CO_3^{2-} \leftrightarrow$ Dolomite	17.09[a]
$Fe^{3+} + 3H_2O - 3H^+ \leftrightarrow$ Ferrihydrite	−4.891[a]
$Pb^{2+} + HS^- - H^+ \leftrightarrow$ Galena	12.78[a]
$Al^{3+} + 3H_2O - 3H^+ \leftrightarrow$ Gibbsite	−8.11[a]
$Ca^{2+} + SO_4^{2-} + 2\,H_2O \leftrightarrow$ Gypsum	4.58[a]
$K^+ + 3Fe^{3+} + 2SO_4^{2-} + 6H_2O - 6H^+ \leftrightarrow$ Jarosite	9.21[a]
$Ni^{2+} + HS^- - H^+ \leftrightarrow$ Millerite	8.042[a]
$Cd^{2+} + CO_3^{2-} \leftrightarrow$ Otavite	12.1[a]
$Fe^{2+} + CO_3^{2-} \leftrightarrow$ Siderite	10.45[c]
$H_4SiO_{4(aq)} - 2H_2O \leftrightarrow SiO_{2(am)}$	3.018[a]
$Zn^{2+} + CO_3^{2-} \leftrightarrow$ Smithsonite	10.0[a]
$Zn^{2+} + HS^- - H^+ \leftrightarrow$ Sphalerite	11.618[a]
$U^{4+} + 2H_2O - 4H^+ \leftrightarrow$ Uraninite	4.85[d]

[a] Source: WATEQ4F.
[b] Source: MINTEQA2.
[c] Source: Singer and Stumm, 1970.
[d] Source: WISMUT.

4.2.4. Neglected processes

The dissolution of aluminosilicate minerals may also be a pH-buffering mechanism of significance in mine tailings. Reports of mine drainage water with elevated concentrations of dissolved silica and aluminum are common (Dubrovsky et al., 1984; Morin et al., 1988; Blowes et al., 1992; Glynn and Brown, 1996). These minerals, however, are slow to dissolve above a pH of 3–4 and may therefore not contribute significantly to the attenuation of the metals of concern, which are mobile below pH = 4. In addition, site-specific data supporting the dissolution of Al-silicates were limited, and pH-buffering by aluminosilicates was excluded. The model, however, allows the inclusion of these processes (Mayer et al., 1999).

Trace quantities of organic matter were also detected in analyses of rock from the aquifer (Table 1). The effect of organic matter on the redox state of the aquifer was neglected, because information about the nature of the material was not available. In sufficient quantity and distribution, reactive organic matter may serve as a redox buffer for the aquifer, enhancing the stability of uranium in the aquifer and providing a sorptive medium for dissolved U.

Ion exchange and sorption reactions may lead to an additional attenuation or release of major cations and heavy metals. However, site-specific ion exchange or sorption parameters, which would justify the quantitative description of these reactions, were not available. Additional contaminant attenuation may be of particular significance, if iron-oxide mineral phases, such as ferrihydrite, are present in the aquifer.

5. Model parameters and setup

A fundamental challenge to the modelling is that detailed information on the trace mineralogy that is expected to control the evolution of the mine water to a significant extent is not available, and is not expected to become available in the near future. The only option, therefore, is to treat the modelling as a sensitivity analysis, with the geochemical parameters that are expected to be controlling as variables. The geochemical modelling will reveal the actual controlling parameters and demonstrate the evolution of the aquifer geochemistry under a range of possible conditions.

5.1. Physical parameters

The 1D reactive transport model extends from the northern end of the mine (Fig. 1) for a distance of 1000 m in the downgradient direction along the short flow section. The physical and hydrogeological conditions for this section are shown in Table 4.

5.2. Geochemical parameters

5.2.1. Source zone geochemistry

In preparation for decommissioning the Königstein mine, a limited flooding experiment was conducted from 1993 until present to evaluate how water draining from the flooded mine workings evolve (Grundwasserforschungsinstitut Dresden, im Auftrag der

Table 4
4th aquifer hydrogeological parameters for short flow section (WASY, 1995)

Parameter	Value
Domain length	1000 m
Domain width	1-D, 1 m unit width
Hydraulic conductivity	1×10^{-5} m s^{-1}
Hydraulic gradient	0.117
Particle velocity	182.5 m $year^{-1}$
Porosity	0.19
Bulk density	2.1 g cm^{-3}
Diffusion coefficient	1×10^{-9} m^2 s^{-1}
Simulation time	100 years

WISMUT, 1998). The source-water chemistry is based upon data collected in the mine during the flooding experiment, 190 days after the experiment began (Table 5). MINTEQA2 calculations indicate that this water is supersaturated with respect to jarosite and silica and is undersaturated with respect to other minerals identified as potentially significant to the geochemical evolution of the water (carbonate minerals, sulfide minerals, gibbsite, ferrihydrite, $Cr(OH)_3$, uraninite, gypsum). MINTEQA2 was used to determine the source water chemistry for the reactive transport modelling by equilibrating the flooding water with the supersaturated mineral phases (Table 5). The source water is acidic and oxidizing, with a measured pH of approximately 2.3 and a calculated pe of approximately 13.5 (Eh = 765 mV), estimated using the Fe(II)/Fe(III) redox couple. The water also contains moderate to high concentrations of dissolved Fe, U, heavy metals and SO_4. This equilibrated water composition is used in all of the reactive transport simulations.

5.2.2. Aquifer aqueous geochemistry

The initial condition aqueous geochemistry of the 4th aquifer was derived from a representative well (HG 7013) located mid-way between the mine workings and the River Elbe. Water collected from this well on Feb. 15, 1996 was assumed to be representative of general water quality in the 4th aquifer (Table 5). MINTEQA2 calculations indicate that this background water is undersaturated with respect to mineral phases considered to be important to the future evolution of the water (uraninite, carbonate minerals, sulfide minerals, gibbsite, ferrihydrite, $Cr(OH)_3$, gypsum, jarosite and silica; Table 6). The measured field chemistry of the aquifer is indicated in the last column of Table 5. For modelling, the initial background aquifer chemistry is determined at the start of each simulation by equilibrating this groundwater water composition with respect to the particular primary minerals involved in the sensitivity analysis.

5.2.3. Aquifer mineralogy

The mineralogy of the aquifer at the Königstein site has been characterized with respect to principal aluminosilicate minerals. Uranium ore is present in the 4th aquifer, downgradient of the mine workings at concentrations of 10 to 20 g $tonne^{-1}$, but local

Table 5
Source and background water composition

Element	Source (unequilibrated)[a]		Source (equilibrated)[b]	HG 7013 water[c]
	mg l^{-1}	mol l^{-1}	mol l^{-1}	mg l^{-1}
Al	176	6.52×10^{-3}	6.57×10^{-3}	n/a
Ca	467	1.16×10^{-2}	1.17×10^{-2}	7.4
Cd	0.99	8.78×10^{-6}	8.85×10^{-6}	n/a
Cl	461	1.30×10^{-2}	1.31×10^{-2}	32.8
Total CO_3	0.01	1.67×10^{-7}	1.01×10^{-8}	82.6
Cr	0.85	1.64×10^{-5}	1.64×10^{-5}	n/a
Fe(II)	15.0	2.69×10^{-4}	1.36×10^{-4}	total Fe = 0.17
Fe(III)	598	1.07×10^{-2}	1.06×10^{-2}	n/a
H_4SiO_4	154	1.60×10^{-3}	9.33×10^{-4}	6.77
K	4.20	1.07×10^{-4}	5.79×10^{-7}	81.8
Mg	49.0	2.02×10^{-3}	2.03×10^{-3}	4.1
Na	548	2.38×10^{-2}	2.40×10^{-2}	41
Ni	6.60	1.12×10^{-4}	1.13×10^{-4}	n/a
Pb	0.10	4.83×10^{-7}	4.86×10^{-7}	n/a
PO_4	7.90	8.32×10^{-5}	8.38×10^{-5}	0.06
SO_4	5071	5.28×10^{-2}	5.30×10^{-2}	26
U(IV)	n/a	n/a	10^{-25}	n/a
U(VI)	48.0	1.78×10^{-4}	1.78×10^{-4}	0.0454
Zn	100	1.53×10^{-3}	1.54×10^{-3}	0.011
pH	2.3		2.3	6.6
pe	13.5		13.3	3.5

[a] From location C-02, 190 days after the start of the flooding experiment (Grundwasserforschungsinstitut Dresden, im Auftrag der WISMUT GmbH, 1998).

[b] Based on observed source water (columns 2, 3), equilibrated with respect to K-jarosite and silica (4th column), pH and pe held constant.

[c] Measured composition of uncontaminated water at well HG 7013 in the 4th aquifer (02/96). The composition of background water in the aquifer is determined by MIN3P at the start of each simulation by equilibrating this 'seed' composition with primary minerals phases present (e.g. one of calcite, ferrihydrite, calcite + ferrihydrite or calcite + pyrite).

maximum concentrations reach several hundred grams per tonne (Table 7). For simplicity, and based on discussion with WISMUT engineers, the ore is assumed entirely uraninite, UO_2, a reduced form of uranium. In the simulations, it is assumed that uraninite is present at a uranium concentration of 20 ppm, and that water in the aquifer is initially at equilibrium with respect to uraninite. No secondary uranium minerals were identified as potential sinks for dissolved U. Whole rock analyses indicate that small amounts of Cd are present in the aquifer material. In the simulations, otavite is considered a primary mineral source of Cd. The mass of otavite is very small (1/1000 to 1/10,000 of the total carbonate content) in comparison to the estimated total carbonate content of the aquifer. Because the host material is a quartz-sandstone, amorphous silica (am-SiO_2) is assumed present in infinite supply and able to precipitate or dissolve at any time to maintain equilibrium.

Minerals which are not present in the aquifer initially, but which may precipitate (and later dissolve) as equilibrium conditions dictate, include gibbsite ($Al(OH)_3$), $Cr(OH)_3$,

Table 6
Saturation state of aquifer water at well HG 7013, determined with MINTEQA2 (based on aquifer water chemistry indicated in last column of Table 5)

Mineral	Initial condition (log SI)
All carbonates	undersaturated (< -2)
Gibbsite	undersaturated (-1.1)
Ferrihydrite	undersaturated (-0.7)
Jarosite	undersaturated (-9.4)
Uraninite	undersaturated (-4)
Gypsum	undersaturated (-3.0)
am-SiO_2	undersaturated (-1.0)
Sulfides	undersaturated

$Ni(OH)_2$, anglesite ($PbSO_4$), and smithsonite ($ZnCO_3$). These minerals serve as sinks for dissolved Al, Cr, Ni, Pb and Zn contained in the source water (Table 7). Jarosite and ferrihydrite are included to serve as potential mineral sinks for dissolved Fe, and gypsum as a sink for SO_4. This list of potential sinks for dissolved metals is intended to be representative of conditions at the site, though not exhaustive or unique.

5.3. Reactive transport sensitivity analyses

Because the available data are not sufficient for predictive modelling, this study has been conducted as a sensitivity analysis to evaluate potential future conditions, which may develop as a result of the flooding of the mine. As discussed in the conceptual model, pH buffering minerals (e.g. carbonates, Al and Fe(III) hydroxides) and redox buffering minerals (sulfides, certain carbonates and hydroxides) are important to the movement of low pH water and dissolved metals, whether they are present as primary minerals or as secondary reaction products. As quantitative data on these minerals are not available, their presence in the aquifer is a variable in the sensitivity analysis. In an effort to probe the influence of these minerals, a large number of simulations have been conducted in the framework of the sensitivity analysis. Of these simulations, five

Table 7
Potential mineral source-sinks for dissolved metals in the background-zone of the 4th aquifer

Element	Possible source minerals	Elemental mass	Possible sink minerals
Al	Gibbsite	1% as Al_2O_3	gibbsite, jurbanite
Cd	Otavite	0.5 ppm Cd	otavite
Cr	None	0	$Cr(OH)_3$
Fe	pyrite, siderite	Up to 2 wt.% as pyrite	pyrite, siderite, ferrihydrite
Ni	Millerite	4 ppm Ni	$Ni(OH)_2$
Pb	Galena	3 ppm Pb	anglesite
U	Uraninite	4 to 640 ppm	uraninite
Zn	Sphalerite	20 ppm Zn	smithsonite, sphalerite

representative cases have been selected to illustrate the profound effect of the trace mineralogical composition on metal mobility.

The first simulation ("conservative") is representative for conditions where the aquifer is devoid of reactive mineral phases. This conservative mass transport simulation provides a basis of comparison for the mobility of the components of interest, under the influence of geochemical reactions. For the remaining simulations, mineralogical parameters are varied within the bounds delineated by the field data and include the initial mass of carbonate minerals (0.2 wt.% calcite: "calcite"-simulation), the presence of oxidized phases (1 wt.% total Me–OH as ferrihydrite, "ferrihydrite"-simulation), the combined presence of calcite and ferrihydrite ("calcite + ferrihydrite"-simulation) and the combined presence of calcite and sulfide mineral phases (1 wt.% pyrite and trace Me-sulfides, "calcite + pyrite"-simulation) in the aquifer (Table 8). For the purposes of this comparison, the sensitivity of plume development to which secondary minerals form as the mine water moves through the aquifer was not evaluated.

5.4. Numerical parameters

In the simulations, time stepping was adaptive, starting at a small value (10^{-10} year) and increasing to a maximum of 0.25 years if convergence was obtained. The average time step varied between 10^{-3} and 10^{-1} years depending on the simulation, with an average step of 10^{-2} years. The model domain was discretized into between 120 and 150 cells, depending on the simulation. One hundred years was selected as a reasonable duration of the simulations. Longitudinal dispersion was neglected in this study to avoid scale-dependent inconsistencies in the model results induced by the occurrence of geochemical reactions on a local scale and the definition of dispersivities on a macro-scale. Although a fully implicit time stepping scheme is used, the effect of numerical dispersion is negligible for reactive species due to the self-sharpening nature of the reaction fronts (Mayer, 1999). For non-reactive species, numerical dispersion was minimized using a VanLeer Flux limiter (van Leer, 1974; Unger et al., 1996). The long-term effect of numerical dispersion on conservative species in the simulations for the "Short Section" is negligible, because several pore volumes pass through the domain during the simulation period.

Table 8
Reactive transport sensitivity analyses

Simulation	Composition	Quantity (wt.%)
"Conservative"	non-reactive	n/a
"Calcite"	carbonate present	0.2 wt.% calcite
"Ferrihydrite"	Me-oxides present	1 wt.% ferrihydrite
"Calcite + ferrihydrite"	carbonates and Me-oxides present	0.2 wt.% calcite 1 wt.% ferrihydrite
"Calcite + pyrite"	carbonates and Me-sulfides present	0.2 wt.% calcite, 1 wt.% sulfides and trace sulfides

6. Simulation results

6.1. Geochemical profiles

Fig. 3 is a typical geochemical profile for the "Long Section" of the aquifer after 50 years of reactive transport. Pyrite and calcite are the primary mineral phases considered present in the aquifer for this simulation. Other scenarios and mineral compositions (see preceding section) are equally likely. Comparisons between the different scenarios will be made in a later section. In general, aqueous concentrations are reported as total aqueous component concentrations and include the contributions of all dissolved species containing the particular component. Solids are reported in terms of their volume fractions in the aquifer.

Fig. 3 clearly shows the effects of pH and pe buffering, sequential secondary mineral precipitation and dissolution and dissolved metal attenuation. Downgradient from the source zone, the pH increases stepwise with plateaus at approximately pH 2, 4, 5 and 6. These pH plateaus represent areas in the aquifer where, after 50 years, the pH of infiltrating source water is buffered upward by the dissolution of secondary gibbsite (pH $\sim$ 4) and siderite (pH $\sim$ 5), and primary calcite (pH $\sim$ 6). The pH 2 zone represents

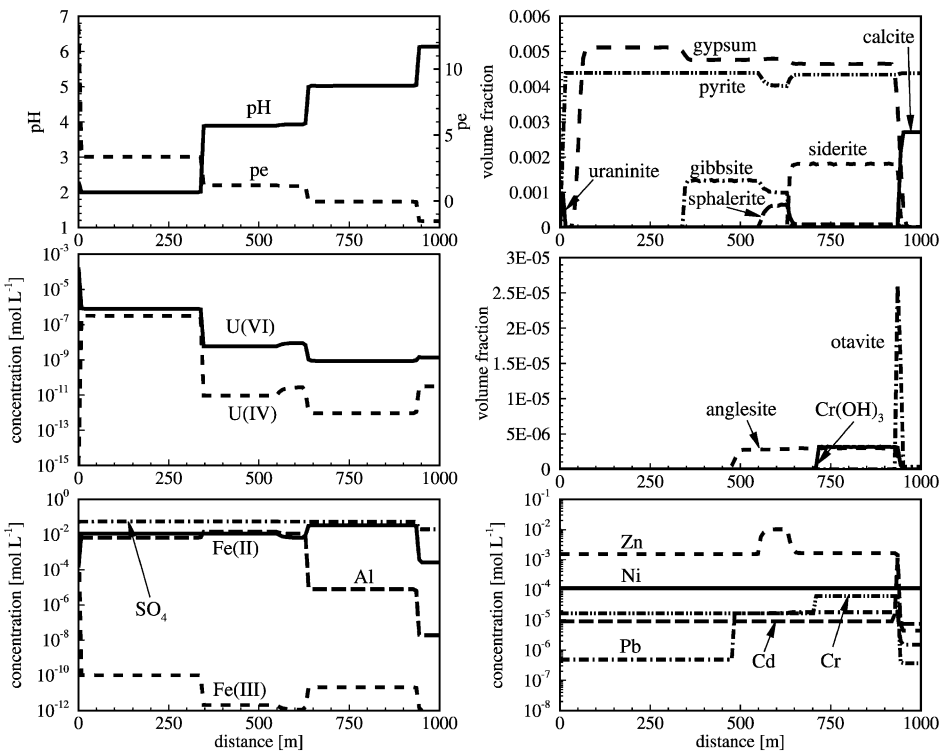

Fig. 3. Simulated concentration profiles along the aquifer after 50 years, for the scenario where the aquifer contains trace amounts of calcite and pyrite.

unbuffered source water, where pH buffering minerals have been depleted. Al concentrations decrease from source values at ~600 m, due to the precipitation of gibbsite at the siderite dissolution front. Fe concentrations decrease at ~950 m, due to the precipitation of siderite at the calcite dissolution front. High sulfate concentrations also lead to the formation of secondary gypsum.

Anglesite, sphalerite, $Cr(OH)_3$, and otavite also precipitate and dissolve, although at much lower volumes than the mineral phases containing major ions. These pH- and pe-controlled mineral dissolution and precipitation reactions result in the observed attenuation of dissolved Pb, Zn, Cr, and Cd, respectively. MINTEQA2 calculations suggest that Cr(III) is mobile under the pH and pe conditions of the source water, and that this water is undersaturated with respect to $Cr(OH)_3$. Under the predicted lower pe and higher pH conditions within the aquifer, the water becomes supersaturated with respect to $Cr(OH)_3$. Cr(VI) was excluded from the simulations because MINTEQA2 calculations suggest that chromium occurs primarily in its reduced state under the simulated range of pH and pe conditions. Continual dissolution and re-precipitation of these secondary minerals also results in the generation of narrow zones of very high concentrations of dissolved metals. In this simulation, Ni moves conservatively.

The figure also demonstrates the important limitations on the transport of dissolved U provided by pyrite or other sulfides in the aquifer. Reactions with pyrite (Eq. (10)) decrease the pe of the incoming source water (pe ~ 3) to much more reduced values (pe ~ 3.5). Under these reduced conditions, uraninite is stable and is not depleted from the aquifer. In addition, the simulation results suggest that uranium in the source water is reduced and precipitated when it encounters pyrite in the aquifer, sharply limiting the transport of dissolved U in the aquifer. The results suggest that after 100 years, pyrite depletion from the aquifer is negligible. Due to the persistence of pyrite in the aquifer, U is attenuated for more than 100 years. The stepwise downgradient decrease in pe primarily reflects decreasing Fe(III) concentrations in the water as higher pH conditions are encountered and as Fe(II) is released due to secondary siderite dissolution.

6.2. Geochemical breakthrough

The simulation results presented in Fig. 4 compare the arrival of the contaminants at a breakthrough point located 1000 m downgradient of the mine for the five simulations considered in the framework of the sensitivity analysis for the "Short Section". Simulations were conducted over a time period of 100 years. Due to the high groundwater velocity in the aquifer, conservative species migrate through the 1000-m section in less than 6 years. The following discussion will focus exclusively on key geochemical parameters and the contaminants of concern.

6.2.1. pH

In the three simulations containing calcite, calcite dissolution buffers the pH to near-neutral for about 55 years. Afterward, the pH decreases sharply in a number of steps (pH 6, 5 and 4), representing the sequential dissolution and eventual depletion of calcite, siderite and gibbsite in the aquifer. Comparing the simulation results shows that

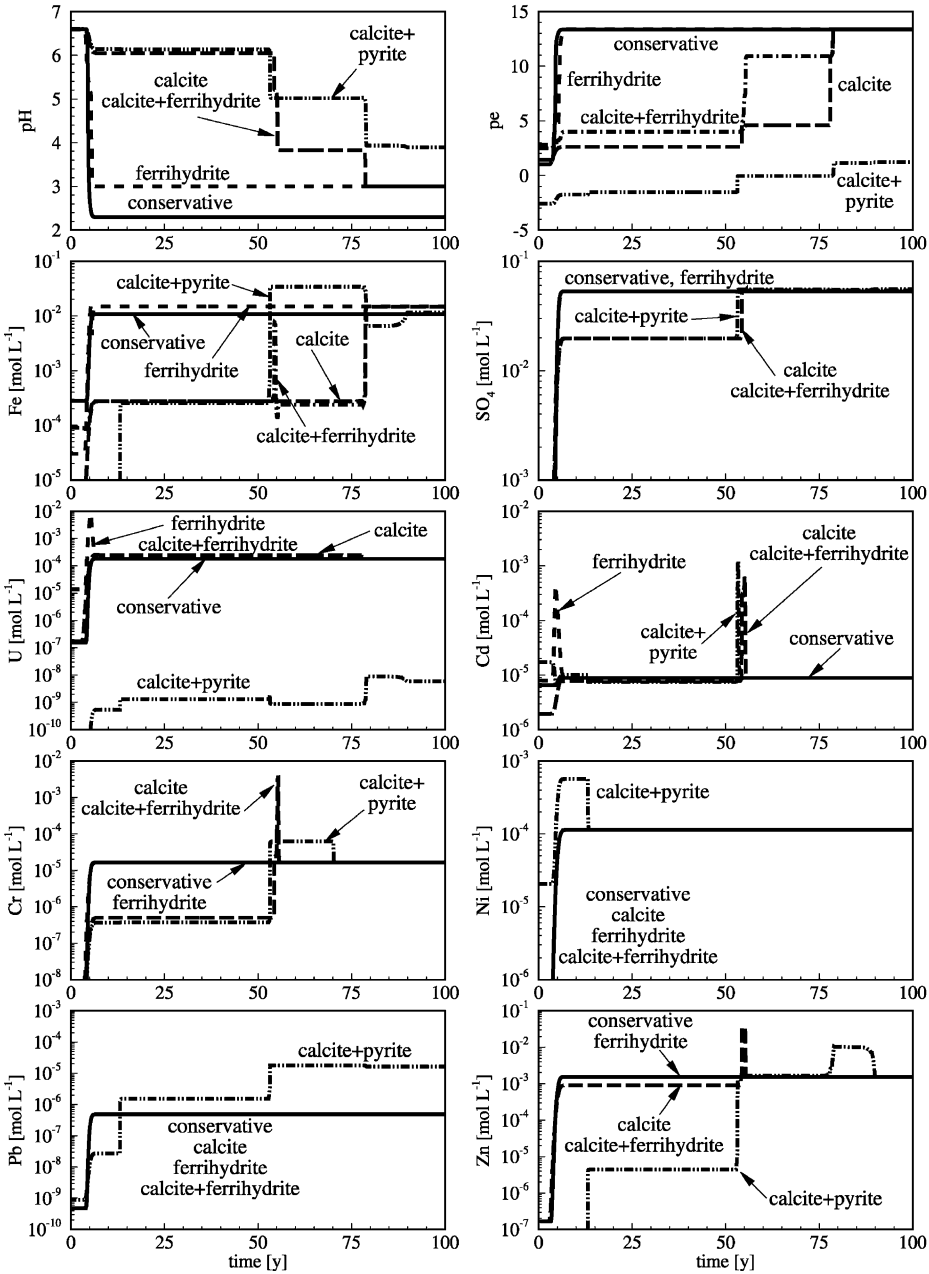

Fig. 4. Breakthrough profiles at $x = 1000$ m for selected components.

the pH plateaus occur at and persist over different periods, due to the formation of differing masses of secondary minerals. For example, the period when the pH is buffered (near pH 5) is extensive in the calcite + pyrite simulation, due to the additional Fe available from the oxidation of pyrite for the formation of secondary siderite. In the calcite and calcite–ferrihydrite simulations, the Fe(II) concentration is limited to that available in the source water, hence, less secondary siderite accumulates. A pH 3 plateau occurs after 80 years in the calcite and calcite–ferrihydrite simulations, due to the dissolution of primary and/or accumulated secondary ferrihydrite. In the case where only ferrihydrite is present initially, the pH decreases to about 3 at 6 years, representing pH buffering by the dissolution ferrihydrite initially present in the aquifer. The mass of ferrihydrite in the aquifer is sufficient to buffer the pH near 3 for more than 100 years. Comparing the reactive transport simulations to the conservative case shows the strong attenuation potential for low pH-waters in the presence of small quantities of pH and Eh buffering mineral phases.

6.2.2. pe

In all cases, the pe increases over time at the end of the section, due to the depletion of mineral phases. The presence of pyrite decreases the source water pe (reduces Fe(III) and U(VI) in the source water), over the 100-year duration of the simulation. The lower oxidizing capacity of the source water decreases the capacity of the water to dissolve metal-bearing minerals in the aquifer. The results also indicate that the dissolution of secondary siderite limits the movement of the high pe conditions in the calcite and calcite–ferrihydrite simulations. When ferrihydrite is present as a redox-buffering mineral, oxidized groundwater reaches the observation point.

6.2.3. Fe

For all simulations where primary Fe-containing mineral phases are present, maximum Fe concentrations are higher than in the conservative case. In the ferrihydrite simulation, the dissolution of ferrihydrite by low pH source water results in the breakthrough of water with Fe concentrations in excess of the source water concentrations as conservative breakthrough occurs. Fe movement is most attenuated and breakthrough concentrations are lowest in the calcite simulation. In all cases where calcite and iron-containing mineral phases are initially present, increases in Fe concentrations are observed after calcite is depleted. These higher Fe-concentrations can be attributed to the dissolution of secondary siderite.

6.2.4. SO_4

The simulation results suggest that the movement of dissolved SO_4 is sensitive to the presence of carbonate minerals in the aquifer. As calcite dissolves, the release of Ca to the water results in saturation of the water with respect to gypsum. Gypsum precipitation limits the dissolved SO_4 concentration to 0.02–0.05 mol l^{-1} in the aquifer downgradient of the gypsum precipitation front (Fig. 4). Greater initial masses of calcite in the aquifer will result in greater attenuation of SO_4. When carbonate minerals are not present, SO_4 transport is conservative (Fig. 4).

6.2.5. U

At low pH and high pe values, uranium is predominately in the mobile oxidized state (U(VI)). At lower pe values, reduced U(IV) is dominant and the mobility of uranium is limited by the solubility of uraninite. The movement of uranium is sensitive to the presence of carbonate minerals, Fe- and Al-oxyhydroxides and sulfides in the aquifer. The uraninite mass in the aquifer is oxidized and dissolved by source water with high Fe(III) and low U(VI) concentrations. Where carbonates or gibbsite are present, the precipitation of Fe(III) as $Fe(OH)_3$ limits the extent of uraninite depletion. The release of U(VI) is greater when ferrihydrite is present and other pH-buffering phases are absent, due to the higher concentration of Fe(III) in the water. The uraninite mass in the aquifer is also important, because the total uranium flux out of the section depends on the mass of uraninite available. Compared to other minerals, the initial mass of pyrite in the simulations (2 wt.%) is high and pyrite is very persistent. As a result, reducing conditions predominate, leading to the reduction of infiltrating dissolved U(VI), the precipitation of uraninite and the removal of uranium from solution.

6.2.6. Cd

In the three simulations where calcite is present, the pH buffering provided by calcite dissolution delays the dissolution of otavite (Fig. 3). Consequently, the attenuation of Cd is dependent primarily on the carbonate content of the aquifer. In simulations where calcite was not present to buffer the pH of advancing source water, otavite dissolution was uninhibited. Similar attenuation of Cd is observed in each of the three calcite buffered simulations, indicating that Cd movement is not sensitive to the presence of ferrihydrite or pyrite. In the ferrihydrite simulation, high Cd concentrations pass through the system after only 6 years, indicating conservative transport. The mass of Cd released to the aquifer water over the 100-year period depends on the mass of otavite initially available in the aquifer.

6.2.7. Cr

MINTEQA2 calculations suggest that Cr(III) is mobile under the pH and pe conditions of the source water, and that this water is undersaturated with respect to $Cr(OH)_3$. Under the predicted lower pe and higher pH conditions within the aquifer, the water becomes supersaturated with respect to $Cr(OH)_3$. Chromium movement is attenuated at pH values above 5.2 by the precipitation of $Cr(OH)_3$ (Fig. 3). Source water Cr is attenuated to a similar degree in each of the three calcite-buffered simulations, although the rate and concentration at which the Cr eventually passes through the aquifer differs. Very high concentrations of Cr break through over a short period (< 2 years) in the simulation where calcite and calcite + ferrihydrite are assumed present. The concentrations are two orders of magnitude lower in the calcite + pyrite simulation, but the breakthrough occurs over 17 years. This difference is due to the presence of an extensive siderite buffer zone, which inhibits the dissolution of $Cr(OH)_3$. Cr moves conservatively in the ferrihydrite buffered simulation, because of the lower equilibrium pH of this system (pH $\sim$ 3). Although not examined here, Cr-mobility would also be enhanced in the ferrihydrite simulation, due to the higher Eh values predicted during ferrihydrite dissolution.

6.2.8. Ni

Millerite (NiS) provides a mineral source for Ni only in the calcite + pyrite simulation. $Ni(OH)_2$ is a potential mineral sink for dissolved Ni in all of the simulations. Under the conditions imposed in these simulations, the water never attains saturation with respect to $Ni(OH)_2$. Hence, Ni moves conservatively. In the calcite + pyrite simulation, accessory millerite contained in the aquifer dissolves as a result of the infiltration of low pH, oxidized source water. Ni released from millerite dissolution breaks through at concentrations greater than source levels early in the simulation ($\sim$ 6 years) and ceases when millerite has been depleted from the aquifer ($\sim$ 15 years).

6.2.9. Pb

The movement of Pb is conservative in all but the calcite + pyrite simulation. In this simulation, Pb is initially attenuated and subsequently breaks through at concentrations that are greater than the background (Fig. 3). The movement of Pb is controlled by the dissolution of accessory galena, which occurs after the trace amounts of millerite initially present in the aquifer have been depleted. After galena has been depleted, the dissolution of secondary anglesite releases Pb to the system.

6.2.10. Zn

The simulations indicate that the movement of dissolved Zn is dependent on the presence of calcite, pyrite and sphalerite in the aquifer. Where the pH is buffered by calcite dissolution, secondary smithsonite ($ZnCO_3$) precipitation causes the attenuation of dissolved Zn (Fig. 3).

When sulfides (sphalerite and pyrite) are present, the infiltration of the low pH oxidized mine water leads to oxidative dissolution of sphalerite, releasing Zn to the pore water. As with Ni and Pb, the movement of Zn is indirectly affected by the presence of pyrite, because pyrite consumes much of the oxidation potential of the water, decreasing the potential for sphalerite dissolution. The simulation results also indicate the attenuation of dissolved Zn due to the precipitation of secondary sphalerite if higher pH conditions are encountered.

6.3. Cumulative mass balance

The implications of the assumptions made about the mineralogy of the aquifer on the transport of dissolved metals and SO_4 in the 4th aquifer are compared on cumulative mass breakthrough curves for the 1000-m observation location in the aquifer (Fig. 5). The simulated cumulative mass loadings are presented for a streamtube of 1 m^2 cross-sectional area over a period of 100 years. Fig. 5 shows, in comparison to the conservative case, that the movement of dissolved metals and SO_4 can be significantly affected by the trace mineralogy of the aquifer, even though some of these effects are short lived. For example, the attenuation of heavy metals due to the formation of secondary mineral phases is only of short duration (Cr and Zn). In the presence of accessory sulfide minerals, the cumulative loads of Cr, Ni, Pb and Zn exceed the mass released in the conservative case. The total Cd mass released exceeds the cumulative

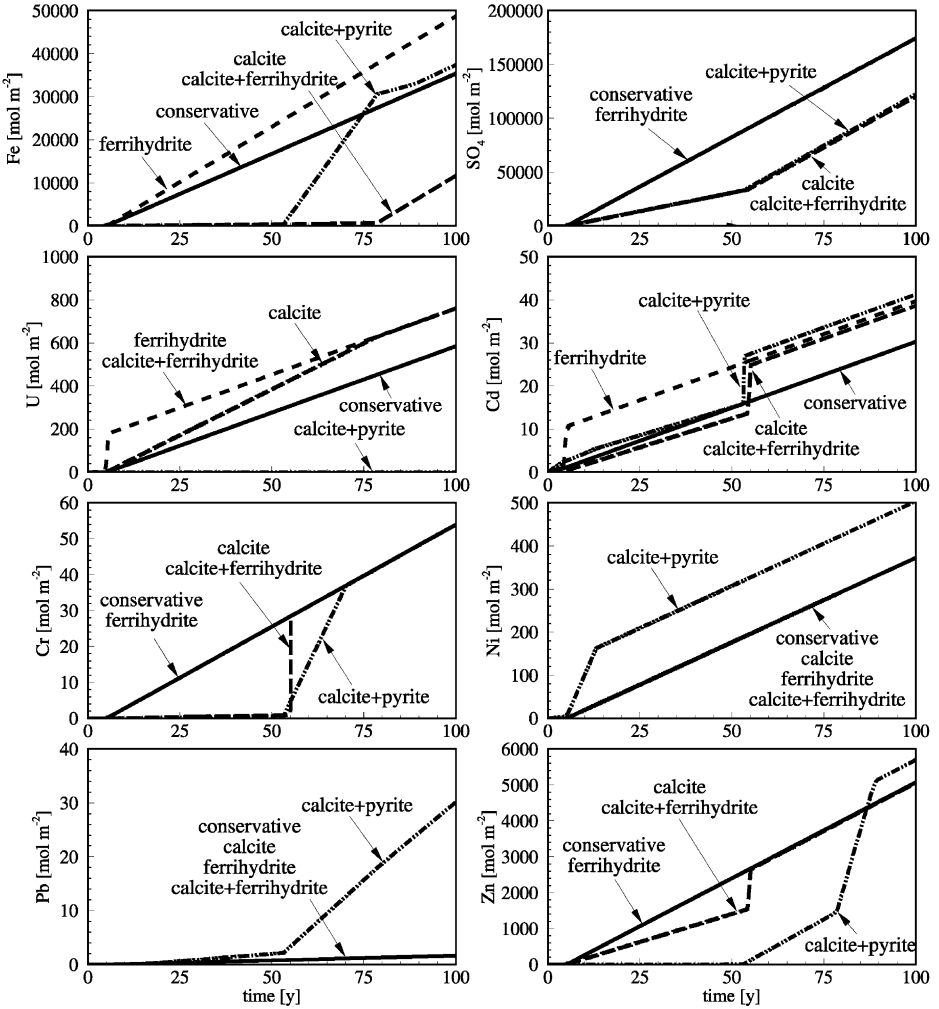

Fig. 5. Mass accumulated at 1000 m in the aquifer, for each of the four aquifer considered aquifer compositions, plus the conservative case.

mass flux of the conservative case for all simulations due to the dissolution of otavite. Similar increased loading of Ni, Pb and Zn occur in the calcite + pyrite simulation, due to the dissolution of millerite, galena and sphalerite. The dissolution of primary ferrihydrite and pyrite can also increase the cumulative iron loading after 100 years compared to the conservative case. A striking example of the influence of trace minerals on the water chemistry is uranium mobility. The results suggest that transport is negligible if the aquifer contains pyrite, but significant if the aquifer is free of sulfides or contains ferrihydrite. The cumulative sulfate mass flux when calcite is present is less than that for the conservative case.

Table 9
Contaminant mass release after 100 years in comparison to conservative case

	Ferrihydrite	Calcite	Calcite + Ferrihydrite	Calcite + Pyrite
Fe	higher	lower	lower	higher
SO_4	equal	lower	lower	lower
U	higher	higher	higher	lower
Cd	higher	higher	higher	higher
Cr	equal	equal	equal	equal
Ni	equal	equal	equal	higher
Pb	equal	equal	equal	higher
Zn	equal	equal	equal	higher

Secondary mineral precipitation may also produce undesirable results at a later time. The simulation results suggest that temporary metal attenuation due to the formation of secondary minerals may lead to later high contaminant concentrations over short periods of time, indicated by rapid increases in the cumulative mass loads (Fig. 5, see also Fig. 4). Table 9 summarizes the results of the mass balance calculations and indicates whether the mass contaminant mass loading is above, below, or equivalent to the loading of the conservative case.

The reactive transport modelling was based on the assumption that the composition of the source water emanating from the mine remains constant over the 100-year simulation period; consequently, the increase in mass for the conservative case is linear.

7. Critical discussion of reactive transport modelling approach

7.1. Benefits

The simulations demonstrate the potential complexity of natural systems. The ability to make the comparisons of geochemically complex transport scenarios is an important benefit of the use of a sophisticated numerical model. Steefel and Van Cappellen (1998) have discussed the advantages of reactive transport models as analysis tools for the investigation of natural systems. Among other important aspects, these authors point out the benefits of mechanistic reactive transport models over empirical models, the potential to use these models to investigate coupled non-intuitive system behavior, the capability to conduct sensitivity analyses investigating possible scenarios and to test conceptual models. The simulations conducted for the Königstein mine site can be used as an illustrative example demonstrating all of these benefits.

The present simulation results indicate that the attenuation potential for low pH-waters and heavy metals is dependent on the trace mineralogy. The geochemical evolution in an aquifer impacted by acid mine drainage can be investigated with a mechanistic reactive transport model taking into account the effect of non-linear coupled processes, but not with an empirical model, for example based on linear retardation factors for the contaminants of concern. The mechanistic formulation used for modelling the König-

stein site was essential for conducting the sensitivity analysis to assess the effect of variations in trace mineralogical composition. This sensitivity analysis allowed identification of the parameters (trace mineralogy) most important to the contamination of the aquifer.

7.2. Limitations

The main limitation of this work is that the simulation results obtained on the basis of the available data cannot be used in a predictive sense. This is primarily due to the temporal and spatial scarcity of the available data. Data limitations involve primarily the very limited information about the mineralogical composition of the aquifer, aquifer heterogeneity, and the composition of the source water. The assumption of primary and potential secondary mineral phases determines the outcome of the simulations; this assumption can be validated only by detailed field sampling. A further source of uncertainty is the chemistry of the source water, which in this case was determined from a flooding experiment. The source water composition affects the depletion of buffer minerals.

A second limitation resides in the model itself. Although the model incorporates all of the controlling physical and chemical processes as far as they can be defined, secondary processes not yet included may also be significant. In addition, it cannot be taken for granted that the database, including equilibrium and solubility constants that the model relies on, is applicable to conditions prevailing at the site. For example, the model uses thermodynamic data for pure-phase minerals, thus the presence of solid-solutions with differing solubilities will affect the mobility of some of the dissolved constituents. In addition, kinetic limitations for mineral dissolution–precipitation reactions were ignored in the simulations, primarily due to a lack of data. As was shown in the sensitivity analysis, secondary minerals with favourable sorptive properties (e.g. hydroxides) may precipitate as a result of the infiltration of the mine water into the 4th aquifer. With increased exchange capacity, dissolved metals may be attenuated more extensively than was shown in the current set of simulations. Furthermore, in the vicinity of mineral precipitation and dissolution fronts, porosity changes may significantly affect the aquifer permeability and groundwater velocities. Although MIN3P calculates changes in volume of the pore space, these changes were not used to recalculate groundwater velocities, to avoid introducing another level of non-linearity and thus further raising computing time.

8. Conclusions

This paper demonstrates the usefulness of conducting reactive transport modelling as a tool for evaluating mine decommissioning and rehabilitation options. The sensitivity analysis conducted at the Königstein site was taken as an example to show that metal mobility is significantly affected by small differences in the overall composition of the aquifer. The model results illustrate that minor variation in estimates of the mass, composition or distribution of trace minerals in the aquifer will affect the predictability

of potential groundwater contamination. The simulations results also show how rock–water interaction can lead to the attenuation or release of contaminants in aquifers impacted by acidic mine drainage. For the Königstein site, reactive transport modelling proved to be a powerful tool for conducting "what-if" scenarios, which could be used to test and improve the site specific conceptual model and to illustrate the potential effect of the flooding of the Königstein mine on the adjacent aquifer. A model formulation that accounts for the highly non-linear nature of coupled rock–water interaction processes is ideally suited for such an investigation.

While predictive modelling of sites such as Königstein is not yet feasible under the limitations of the presently available mineralogical and source chemistry data, this does not detract from the value of the modelling. Clearly, modelling is the only way to quantify the sensitivity of the system to selected parameters and to give insight into the complex problems of the geochemical evolution of the mine water, under the conditions of flooding. This insight allows us to better understand the potential for contamination at the site and to evaluate possible closure options.

Notation

Symbol	Description
D_a	dispersion tensor ($m^2\ s^{-1}$)
N_c	number of components (–)
N_m	number of minerals (–)
Q_j^{in}	internal source-sink term (mol l^{-1} bulk s^{-1})
Q_j^{ex}	external source-sink term (mol l^{-1} bulk s^{-1})
R_i^m	dissolution–precipitation rate (mol l^{-1} bulk s^{-1})
T_j^a	total aqueous component concentrations (mol l^{-1} H_2O)
V_i^m	molar volume of mineral phase (l mineral mol^{-1})
v_a	particle velocity (m s^{-1})
t	Time (s)
ϕ	Porosity (l H_2O l^{-1} bulk)
φ_i	mineral volume fraction (l mineral l^{-1} bulk)

Acknowledgements

This paper arose out of an industrial research contract awarded to the University of Waterloo by WISMUT of Chemnitz, Germany. The work was also supported by the Natural Sciences and Engineering Research Council of Canada (NSERC) through operating grants to D.W. Blowes and E.O. Frind, and by a Government of Canada Scholarship held by K.U. Mayer.

References

Allison, J.D., Brown, D.S., Nova-Gradac, K.J., 1991. MINTEQA2/PRODEFA2, A Geochemical Assessment Model for Environmental Systems: Version 3.0 User's Manual. Environmental Research Laboratory, Office of Research and Development, U.S. EPA, Athens, GA, 106 pp.

Bain, J.G., Blowes, D.W., Robertson, W.D., Frind, E.O., 2000. Modelling of sulfide oxidation with reactive transport at a mine drainage site. Journal Of Contaminant Hydrology 41 (1–2), 23–47.

Ball, J.W., Nordstrom, D.K., 1991. User's manual for WATEQ4F, with revised thermodynamic data base and test cases for calculating speciation of major, trace and redox elements in natural waters. U.S. Geological Survey, Open-File Report 91-183, 189 pp.

Blowes, D.W., Jambor, J.L., Appleyard, E.C., Reardon, E.J., Cherry, J.A., 1992. Temporal observations of the geochemistry and mineralogy of a sulfide-rich mine-tailings impoundment, Heath Steele Mines, New Brunswick. Exploration and Mining Geology 1 (3), 251–264.

Diersch, H.-J.G., 1997. Interactive, graphics-based finite element simulation system FEFLOW for modeling groundwater flow, contaminant mass and heat transport processes. FEFLOW User's Manual Version 4.7, August 1997. WASY Institute for Water Resources Planning and Systems Research, Berlin.

Dubrovsky, N.M., Morin, K.A., Cherry, J.A., Smyth, D.J.A., 1984. Uranium tailings acidification and subsurface contaminant migration in a sand aquifer. Canadian Journal of Water Pollution Research 19 (2), 55–89.

Glynn, P., Brown, J., 1996. Reactive transport modelling of acidic metal-contaminated ground water at a site with sparse spatial information. In: Lichtner, P.C., Steefel, C.I., Oelkers, E.H. (Eds.), Reactive Transport in Porous Media. Reviews in Mineralogy, vol. 34. Mineralogical Society of America, Washington, D.C., pp. 377–438.

Grundwasserforschungsinstitut Dresden, im Auftrag der WISMUT, 1998. Komplexe Auswertung des Flutungsexperimentes und Interpretation im Hinblick auf die geplante Flutung der Grube Königstein. Dresden, Mai 1998. Internal report.

Johnson, R., Blowes, D.W., Robertson, W.D., Jambor, J.L., 2000. The hydrogeochemistry of the Nickel Rim mine tailings impoundment. Journal of Contaminant Hydrology 41 (1–2), 49–80.

Lichtner, P.C., 1996. Continuum formulation of multicomponent–multiphase reactive transport. In: Lichtner, P.C., Steefel, C.I., Oelkers, E.H. (Eds.), Reactive Transport in Porous Media. Reviews in Mineralogy, vol. 34. Mineralogical Society of America, Washington, D.C., pp. 1–81.

Mayer, K.U., 1999. A numerical model for reactive transport in variably-saturated porous media. PhD Thesis, Department of Earth Sciences, University of Waterloo, Waterloo, ON, Canada.

Mayer, K.U., Benner, S.G., Blowes, D.W., 1999. The reactive transport model MIN3P: application to acid mine drainage generation and treatment—Nickel Rim Mine site, Sudbury, Ontario. Mining and the Environment, Conference Proceedings Volume 1, September 13–17, 1999, Sudbury, Ontario, pp. 145–154.

Mayer, K.U., Blowes, D.W., Frind, E.O., 2000. Numerical modeling of acid mine drainage generation and subsequent reactive transport. ICARD 2000 — Proceedings From the Fifth International Conference on Acid Rock Drainage. Society for Mining, Metallurgy, and Exploration, Inc., Littleton, Colorado, pp. 135–141.

Morin, K.A., Cherry, J.A., Davé, N.K., Lim, T.P., Vivyurka, A.J., 1988. Migration of acidic groundwater seepage from uranium-tailings impoundments: 1. Field study and conceptual hydrogeochemical model. Journal of Contaminant Hydrology 2, 217–303.

Parkhurst, D.L., 1995. User's guide to PHREEQC—a computer program for speciation, reaction-path, advective-transport, and inverse geochemical calculations. U.S. Geol. Surv., Water Resources Invest. Report 95-4227.

Plummer, L.N., Prestemon, E.C., Parkhurst, D.L., 1991. An interactive code (NETPATH) for modeling net geochemical reactions along a flow path. U.S. Geol. Surv., Water Resources Invest. Report 91-4078.

Singer, P.C., Stumm, W.J., 1970. Journal of American Water Works Association 62, 198–202.

Steefel, C.I., Lasaga, A.C., 1994. A coupled model for transport of multiple chemical species and kinetic precipitation/dissolution reactions with application to reactive flow in single phase hydrothermal systems. American Journal of Science 294, 529–592.

Steefel, C.I., Van Cappellen, P., 1998. Editorial in 'Special Issue: reactive transport modeling of natural systems'. Journal of Hydrology 209, 1–7.

Unger, A.J.A., Forsyth, P.A., Sudicky, E.A., 1996. Variable spatial and temporal weighting schemes for use in multi-phase compositional problems. Advances in Water Resources 19 (1), 1–27.

van Leer, B., 1974. Towards the ultimate conservative scheme: II. Monotonicity and conservation combined in a second order scheme. Journal of Comparative Physiology 14, 361–370.

Walter, A.L., Frind, E.O., Blowes, D.W., Ptacek, C.J., Molson, J.W., 1994a. Modeling of multicomponent

reactive transport in groundwater: 1. Model development and evaluation. Water Resources Research 30 (11), 3137–3148.

Walter, A.L., Frind, E.O., Blowes, D.W., Ptacek, C.J., Molson, J.W., 1994b. Modeling of multicomponent reactive transport in groundwater: 2. Metal mobility in aquifers impacted by acidic mine tailings discharge. Water Resources Research 30 (11), 3149–3158.

WASY, 1995. Gesellschaft für wasserwirtschaftliche Planung und Systemforschung mbH, Berlin. Stofftransportmodellierung im grossräumigen Bereich um die Lagerstätte Königstein und in der Grube Königstein, Report prepared for WISMUT, Chemnitz, 1995.

Wunderly, M.D., Blowes, D.W., Frind, E.O., Ptacek, C.J., 1996. Sulfide mineral oxidation and subsequent reactive transport of oxidation products in mine tailings impoundments: a numerical model. Water Resources Research 32 (10), 3173–3187.

Yeh, G.T., Tripathi, V.S., 1989. A critical evaluation of recent developments in hydrogeochemical transport models of reactive multichemical components. Water Resources Research 25, 93–108.